Research on Engineering Structures & Materials
www.jresm.org
Research Group

Research Article

Structural behavior of deficient hollow steel columns strengthened using GFRP

P. Sangeetha*,a, R. Prithvi[b], Ashwin Kumaran V[c], Murali B[d], Yaashika M[e]

Department of Civil Engineering, Sri Sivasubramaniya Nadar College of Engineering, Chennai-603 110, Tamil Nadu, India

Article Info

Article History:

Received 21 Nov 2024

Accepted 02 Feb 2025

Keywords:

Hollow steel columns;
Axial compression;
Vertical and horizontal slits;
GFRP wrapping;
Load carrying capacity;
Failure mode

Abstract

This study investigates the axial compression behavior of hollow steel columns (HSCs) with and without defects, specifically horizontal and vertical slits, and strengthened using Glass Fiber Reinforced Polymer (GFRP) wrapping. Twelve specimens were tested for failure under axial compression. The parameter varied in the study are circular and square sections and type of slit. Experimental and finite element analyses (FEA) were performed to evaluate the structural performance of intact and defective columns. The load-carrying capacity HSC with a horizontal slit was increased by 20 % when compared to the control specimen without a slit. GFRP wrapping was applied in three plies to enhance load-bearing capacity by 50 % and mitigate the effects of structural deficiencies. The results demonstrated that GFRP significantly improved the axial load capacity and ductility of the columns, particularly in defective specimens, by reducing stress concentrations around the slits. Failure modes were analyzed, showing delayed local buckling, reduced plastic hinge formation, and controlled rupture or delamination of GFRP layers. FEA simulations in ANSYS replicated the experimental behavior accurately with a minimal error of less than 5%, providing insights into stress distribution, load–axial deflection characteristics, and failure mechanisms. This study underscores the effectiveness of GFRP wrapping as a strengthening technique for improving the performance and reliability of deficient CHSCs.

1. Introduction

During Hollow steel columns are commonly used in structural applications due to their high strength and efficiency in load-bearing. Deficiencies in hollow steel columns can arise from various factors, including manufacturing defects, wear and tear, or intentional modifications like slits for utility passages. These defects can lead to stress concentrations and local buckling, reducing the columns' load-carrying capacity and overall stability. The defects such as vertical and horizontal slits can significantly impair their structural performance. There were many techniques available to strengthen the hollow steel tube. FRP composites are extensively applied in structural engineering due to their superior strength-to-weight ratio, corrosion resistance, and adaptability. They are widely used in the retrofitting and strengthening of structural members. FRP commonly enhances flexural and shear capacities. In columns, it provides confinement, boosting axial strength and ductility. For dapped ends and corbels, FRP reinforcement alleviates stress concentrations and cracking, thereby increasing the load-carrying capacity. One promising solution to enhance the strength and stability of these deficient columns is to use glass fiber-reinforced polymer (GFRP) for strengthening. The advantages of GFRP wrapping compared to other techniques are listed in Table 1. GFRP has been extensively researched as a retrofitting material due to its high strength-to-

*Corresponding author: sangeethap@ssn.edu.in
[a]orcid.org/0000-0002-7630-011X; [b]orcid.org/0009-0003-9314-9428; [c]orcid.org/0009-0003-3045-1320; [d]orcid.org/0009-0008-3641-5204; [e]orcid.org/0009-0007-4203-1058
DOI: http://dx.doi.org/10.17515/resm2025-541st1121rs

weight ratio, corrosion resistance, and ease of application. Researchers have found that GFRP wrapping can effectively improve the structural performance of deficient columns. Mohammad et al. [1], experimental and numerical studies have been conducted on the structural behaviours of steel square hollow section (SHS) compression members with initial horizontal or vertical deficiencies, which were reinforced using Carbon Fiber Reinforced Polymer (CFRP) sheets. Similarly, another study by Rao et al. [2] demonstrated that GFRP strengthening enhanced the stiffness and delayed the onset of buckling in deficient hollow steel columns. The effect of CFRP strengthening of the deficient steel SHS columns was studied under axial compression and reported that CFRP wrapping improves the strength of column and reduces the local deformation at the places of deficient [3]. Experimental and numerical investigation on vertical and horizontal deficient SHS columns strengthened with CFRP was done and found that strength lost due to deficient was regained and delay the local buckling after strengthening [4]. The effects of axial loading, stiffness, axial displacement, the position and shape of deficient region on the length of steel SHS columns, and slenderness ratio are examined through a detailed parametric study by Shahraki et al. [5]. Comparative studies have been conducted to evaluate the effectiveness of various strengthening techniques, including the use of GFRP by Lin et al. [6] & sangeetha et al. [7, 8]. Compared the performance of steel-plated and GFRP-strengthened hollow steel columns and highlighted that GFRP retrofitting was more effective in reducing local deformations and distributing stresses uniformly.

Table 1. Comparison of strengthening methods for hollow steel columns

Method	Advantages of Present Method (GFRP Wrapping)
Concrete Filling	Lightweight and offers confinement with minimal weight addition.
Internal Steel Reinforcements	Easier to retrofit and avoids complex fabrication.
External Steel Plates	Corrosion-resistant, no welding required, and aesthetically better.
CFRP Wrapping	Cost-effective for large applications and provides better ductility.
Steel Jacketing	Lightweight, corrosion-resistant, and easier to retrofit.
Concrete Filling	Lightweight and offers confinement with minimal weight addition.

The effectiveness of CFRP composites and steel plates in retrofitting deficient steel SHS columns under axial compression was studied [9]. The study found that CFRP and steel plates reduce stress in damaged regions and enhance load-bearing capacity, but CFRP outperformed steel plates due to issues like increased weight and welding challenges. Eight specimens were tested and simulated, showing CFRP's superior ability to compensate for cross-section reduction. The failure mode of the CFRP-confined rectangular concrete-filled stainless steel tube stub columns was studied [10]. First, the local rupture of CFRP occurred, and the local buckling failure of the concrete-filled stainless-steel tube was present. The bearing capacity of the CFRP-confined concrete-filled stainless steel tube stub columns was stronger than that of concrete-filled stainless steel tube specimens because of the strong restraint capacity of CFRP. The study explored [11] the effect of CFRP strengthening on the structural behavior of square hollow section steel members having an initial deficiency under combined axial and lateral load. To study the effects of the strengthening, 17 specimens were tested under four loading scenarios, with 12 specimens strengthened using CFRP sheets. Finite Element Analysis (FEA) has been widely used to model and predict the behavior of GFRP-strengthened columns. In the study by Sharma and Singh [12], FEA models were developed to simulate the performance of deficient columns with different GFRP configurations. The models were validated through experimental testing, agreeing with the observed structural responses. The stiffness and strength parameters acquired from 27 numerical simulations were assessed for

Square Hollow Section (SHS) profiles with rectangular apertures, which were subjected to axial displacements and found that the FEA model was effective with a minimal error of 10% [13].

Despite the extensive research on strengthening hollow steel columns, existing studies primarily focus on CFRP wrapping, steel jacketing etc. over the deficient hollow steel columns. Moreover, limited attention has been given to the combined effects of deficiencies, such as vertical and horizontal slits, on the structural behaviour of hollow steel columns strengthen with GFRP wrapping.

2. Materials and Methods

2.1 Material Properties

The coupon test was conducted to evaluate the material properties, from the test, the following details were observed: yield stress at 267 N/mm^2, ultimate stress at 475 N/mm^2, modulus of elasticity at 2.04x10^5 N/mm^2, and elongation after fracture at 48 mm. According to the manufacturer's data for GFRP sheets, the adopted thickness of 1 mm, tensile strength of 1724 MPa, tensile modulus of 76 GPa, elongation after fracture at 2.8%, and mass density of 2500 kg/m^2.

2.2 Experimental Study

The experimental investigation involved subjecting GFRP-wrapped hollow steel columns with and without slits to axial compression to evaluate their load-carrying capacity and deformation behavior. Specimens included circular and square hollow sections with vertical and horizontal slits, both strengthened and unstrengthened with three plies of GFRP wrapping. The columns were tested under monotonic axial loading using a universal testing machine (UTM) at a constant displacement rate. Axial displacement and axial strain were noted using a dial gauge and strain indicator respectively.

Totally Twelve hollow deficient columns were tested to failure under axial compression. The specimens were grouped into four groups such as group A (Unwrapped GFRP Circular section) which includes specimens without any deficient, specimen with vertical deficient and specimens with horizontal deficient. Group B (Wrapped GFRP Circular section), without any deficient, with vertical deficient and with horizontal deficient. Similarly, Unwrapped GFRP Square section and the wrapped GFRP Square section are grouped as group C and group D respectively. Table 1 provides the detailed dimensions of the hollow deficient columns. The vertical deficient (slit) is made parallel to the axis of the column, located at the mid-height of the specimen and the horizontal deficient (slit) is made perpendicular to the column's axis, also centered at mid-height. The dimensions of the horizontal and vertical slit on the hollow specimens are given in Table 2 as (b_s x d_s) which is 50 mm x 15 mm and 15 mm x 50 mm respectively.

Table 2. Description of specimens

Category	Specimen	D/B	t_s	H	t_f	No. of plies
				mm		
Group A	DSCC-NS-NW	76.5	1.8	624	-	-
	DSCC-HS-NW	76.5	1.8	625	-	-
	DSCC-VS-NW	76.5	1.8	623	-	-
Group B	DSCC-NS-GFRP	76.5	1.8	626	1	3
	DSCC-HS-GFRP	76.5	1.8	625	1	3
	DSCC-VS-GFRP	76.5	1.8	624	1	3
Group C	DSSC-NS-NW	76.5	1.8	623	-	-
	DSSC-HS-NW	76.5	1.8	626	-	-
	DSSC-VS-NW	76.5	1.8	627	-	-
Group D	DSSC-NS- GFRP	76.5	1.8	623	1	3
	DSSC-HS- GFRP	76.5	1.8	624	1	3
	DSSC-VS- GFRP	76.5	1.8	625	1	3

To ensure optimal bonding between the GFRP sheets and steel columns, each specimen was sandblasted to remove any rust, oxides, or other contaminants, and cleaned using acetone to obtain a smooth surface. A two-part epoxy resin for bonding GFRP to steel was applied over the prepared surface. For GFRP wrapping, sheets were positioned around the slit region of the columns by covering the whole column including the deficient portion fully. The 3-plies of GFRP fibers wrapping were done for all specimens. GFRP were oriented circumferentially around the column to maximize lateral confinement, counteracting potential buckling in the weakened regions. Once applied, all wrapped specimens were left to cure at room temperature for 48 hours. Fig. 2 shows the specification of the circular and square hollow deficient specimens before testing.

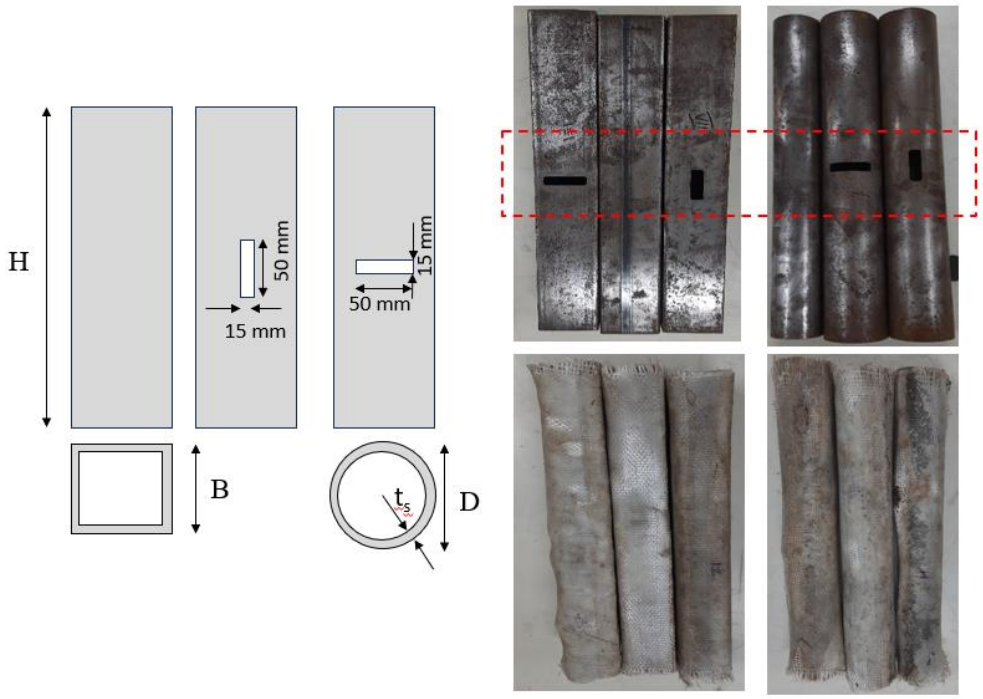

Fig. 2. Specification details of Deficient HSC with and without slit

Table 2. Experimental results and its observation

Specimen	Ultimate load[kN]	Axial deformation[mm]	Observed failure
DSCC-NS-NW	53.0	5	Material yielding + Local buckling
DSCC-HS-NW	73.6	5.8	Local bucking + Yielding near the slit
DSCC-VS-NW	58.1	5.3	Local buckling
DSCC-NS-GFRP	108.0	5.2	Local buckling +Tearing of FRP
DSCC-HS-GFRP	135.0	5.3	Local buckling +Tearing of FRP near slit
DSCC-VS-GFRP	120.0	5.8	Local buckling +Tearing of FRP near slit
DSSC-NS-NW	48.0	2.3	Inward /outward + Local buckling near the slit
DSSC-HS-NW	64.0	2.6	Inward /outward + Local buckling near the slit
DSSC-VS-NW	53.0	2.4	Inward /outward + Local buckling near the slit
DSSC-NS- GFRP	100.0	5.2	Inward /outward + Local buckling with GFRP tearing
DSSC-HS- GFRP	125.0	6.6	Inward /outward + Local buckling with GFRP tearing near the slit
DSSC-VS- GFRP	110.0	6.4	Inward /outward + Local buckling with GFRP tearing near the slit

A universal testing machine (UTM) with a maximum load capacity of 600 kN was used. Specimens were positioned vertically between two steel plates to ensure uniform load application. A dial

gauge with the least count of 0.01 mm was placed along the column height to monitor axial deformation. Strain gauges of 20 mm gauge length were attached near the slit regions to capture local strain distribution. The axial compressive load was applied at a controlled displacement rate of 0.02 mm/min until failure. The schematic diagram of the testing arrangement and specimens under loading in UTM is shown in Fig. 3. Table 2 lists the observations of the tested specimens. The table shows that GFRP wrapping provided a substantial enhancement, with HS-GFRP specimens demonstrating the highest ultimate load in both circular (135 kN) and square sections (125 kN). The ultimate load for DSCC-HS-GFRP (135.0 kN) increased by approximately 83% compared to DSCC-NS-NW (73.6 kN). Similarly, the square column DSSC-HS-GFRP (125.0 kN) showed significant improvement over DSSC-HS-NW (64.0 kN), highlighting the effectiveness of GFRP confinement. GFRP provided enhanced confinement, delaying local buckling and increasing load resistance. However, tearing of the GFRP wrap near slits was observed under peak loads, highlighting areas for material improvement or enhanced application techniques.

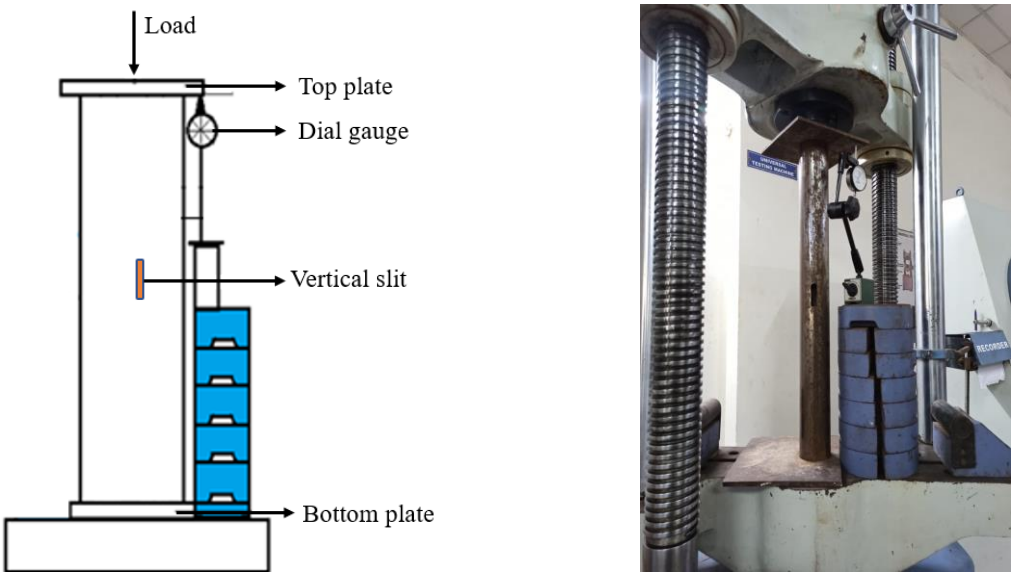

Fig. 3. Arrangement for testing of columns and its schematic diagram

2.3 Analytical Study

The Finite Element Analysis (FEA) was performed using ANSYS version 2024 software, as it is a highly capable FEA tool that excels in modeling complex structures. It offers accurate nonlinear material modeling, reliable meshing, and efficient solver options to simulate real-world behaviours. The steel columns were modelled using SOLID186 elements to capture plasticity and buckling behaviour, while GFRP layers were represented using SHELL181 elements to simulate orthotropic material properties and failure criteria. Material properties derived from experimental tests, including yield stress at 267 N/mm^2, ultimate stress at 475 N/mm^2, Poisson's ratio of 0.3 for steel & tensile strength of 1724 N/mm^2 and elastic modulus of 1724 N/mm^2 for GFRP was given as input for FEA model. Boundary conditions included fixed supports and displacement-controlled axial loading, with bonded contact defining the steel-GFRP interface. The bond state between the steel substrate and the GFRP wrapping plays a critical role in the load-carrying capacity and failure behaviour of specimens. The perfect bond assumption was validated by experimental evidence and numerical stress distributions. The bonded-contact model in the current FEA analysis was supported by experimental evidence and stress transfer patterns. It provides an accurate and reliable representation of the steel-GFRP interaction for the studied specimens, with minimal impact on the overall accuracy of the load predictions. Using the coinciding nodes option in ANSYS the connection between the SOLID and SHELL elements was made and it is an efficient and accurate way to model perfectly bonded interfaces. It enables seamless load transfer and realistic simulation of confinement effects, making it ideal for studying GFRP-wrapped steel or concrete columns under axial loads. The finite element model of the specimen DSCC – NS-NW, DSCC – NS – GFRP, DSSC – HS – NW & DSSC – HS – GFRP are shown in Fig. 4. The finite element model used a finer mesh (2 – 3

mm) for hollow steel column with or without slit and GFRP layers have meshed with element sizes matching their thin geometry (0.5–1 mm per ply). One end of the column is fixed to prevent all translations and rotations ($U_x = U_y = U_z = 0$; displacements in all directions are zero). Applying axial compression at the opposite end, while lateral displacements at the loaded end are constrained. This study utilized nonlinear static analysis in ANSYS to simulate the behavior of hollow steel columns under axial compression. The Newton-Raphson iterative method was employed to solve the nonlinear equations, ensuring accurate convergence through force and displacement criteria. Incremental load steps were applied to capture progressive nonlinear effects, such as material yielding, stress redistribution, and buckling near the slit regions. The experimental results revealed that the tearing of GFRP sheets was predominantly driven by stress concentrations at the slits and areas of local buckling, highlighting the role of GFRP wrapping in delaying failure. The finite element analysis successfully replicated these failure modes, validating the use of the Hashin failure criteria to capture the behavior of the GFRP under axial compression. The FEA results closely matched experimental outcomes, with a minimal error of 3.5% in load-carrying capacity predictions and consistent failure patterns. This approach validated the reliability of the chosen methodology in capturing material and geometric nonlinearities, stress redistribution, and the interaction between steel and GFRP wrapping.

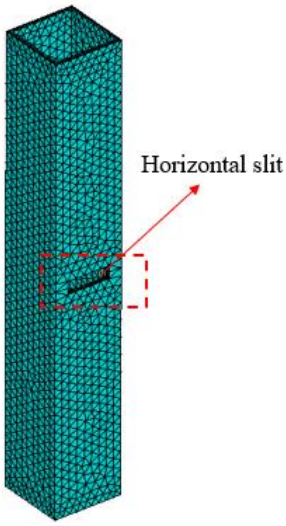

Fig. 4. Mesh model of a deficient hollow column- DSSC-HS-NW

3. Results and discussions

3.1 Load – Axial Compression Behavior of Group A Specimens

The load-axial compression curve of the circular column without a slit, with a vertical slit and with a horizontal slit was shown in Fig. 5. It was noted that the circular columns with vertical slits DSCC – VS – NW show reduction in both stiffness (33 %) and load-bearing capacity. The stiffness is measured by calculating the deflection under an applied load. This may be due to the vertical slit running parallel to the axis of the column, creating a stress concentration along the slit's edges and introducing a weak zone in the load path. This orientation disrupts the distribution of axial stresses, causing the column to be more vulnerable to buckling. The specimen with horizontal slits DSCC – HS – NW primarily affects the column's flexural stiffness and contributes to buckling due to bending or shear forces. Thus, the introduction of either vertical or horizontal slits reduces the ultimate load-bearing capacity of circular columns. However, columns with vertical slits exhibit a more pronounced reduction due to the alignment of the slit along the load path, which leads to a faster decline in the load-bearing capacity of the column.

The failure observed in columns with vertically slit is typically localized around the slit, with local buckling occurring along the slit edges. This causes a rapid loss in load-carrying capacity, resulting in brittle or semi-brittle failure characterized by significant deflection in the slit. Whereas, a column with a horizontally slit fails typically due to a combination of local buckling and yielding near the

slit region. This type of slit often leads to flexural deformation, causing the column to fail in a more ductile manner compared to vertical slits. Fig.6 shows the circular column specimens with vertical and horizontal slits after testing and compared to the control specimen without any deficiency.

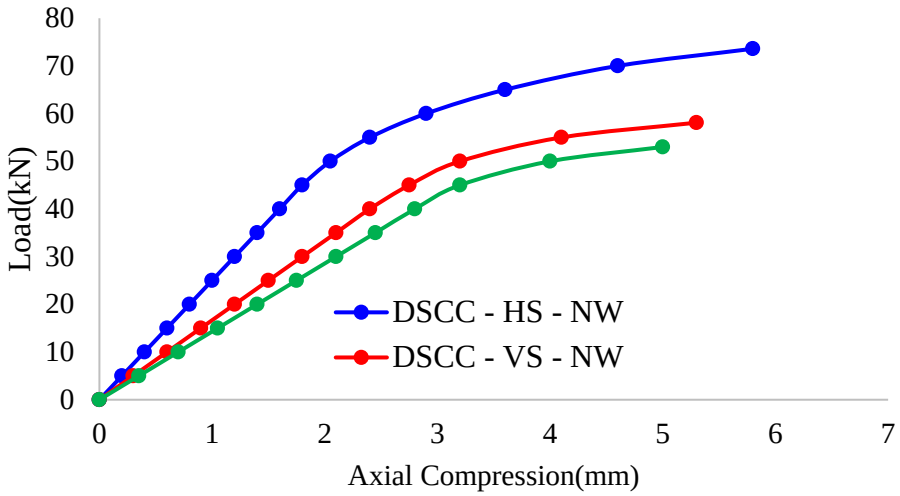

Fig. 5. Load – axial compression behavior of Group A specimens

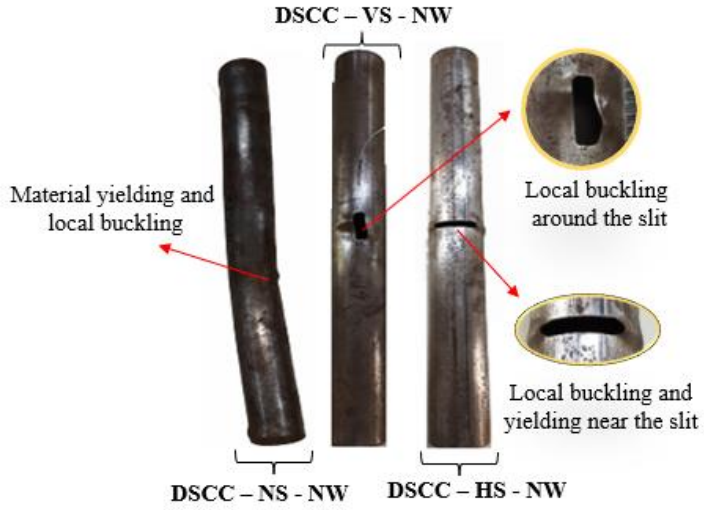

Fig. 6. Circular column specimen with and without deficient after test

3.2 Load – Axial Compression Behavior of Group B Specimens

The load–axial compression behavior of the GFRP-wrapped circular column without a slit, with a vertical slit and with a horizontal slit was shown in Fig. 7. It was noted that GFRP confinement circular column (DSCC – NS – GFRP) increases axial stiffness and allows the column to carry a higher load. The wrapping resists lateral expansion of the steel under compression, allowing the specimen to reach a higher peak load than unwrapped columns without deficiency. In specimen DSCC – HS – GFRP, the horizontal slits do not directly interrupt the load path, the addition of GFRP wrapping further improves load capacity by reinforcing the column's integrity and restricting deformation near the slit. This results in a higher peak load compared to unwrapped columns with horizontal slits. GFRP wrapping acts as a reinforcing layer over the vertical slit, helping to bridge the discontinuity and preventing stress concentrations along the slit edges. The enhancement in resistance of GFRP-wrapped hollow steel columns arises not from the direct compressive resistance of GFRP but from its ability to confine, restrain, and redistribute stresses in the steel. This results in an improved load-bearing capacity compared to unwrapped columns with vertical slits.

Fig.8 shows the column specimens after testing. From the test column specimens, it was observed that local buckling with tearing of the GFRP sheet around the vertical and horizontal slit.

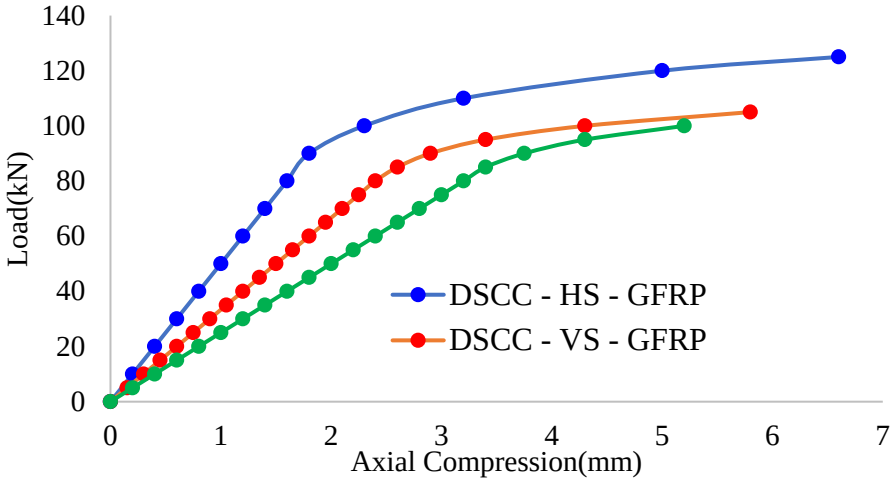

Fig. 7. Load – Axial compression behavior of Group B specimens

Fig. 8. Failure mode of the GFRP wrapped circular column with and without deficient

3.3 Load – Axial Compression Behavior of Group C Specimens

Fig. 9 shows the load–axial compression behavior of the unwrapped square column with or without deficiency. It is inferred from the curve, that the load-carrying capacity of DSSC-HS-NW is 25 % more than the control specimen DSSC-NS-NW. This may be due to the redistribution of load; the presence of a horizontal slit alters the load path and improves the load-carrying capacity. Similarly, the increase in the load-carrying capacity of 9 % was recorded for specimen DSSC-VS-NW as compared to DSSC-NS-NW. All the square hollow specimens fail mainly by inward and outward local buckling and also observed slight distortion around the vertical and horizontal slit. Fig. 10 shows the failure model of the unwrapped square hollow deficient column. The parameters investigated in Figure 10 are buckling patterns, with a focus on identifying regions of local and global buckling to understand the slit configurations which influence failure modes in specimens DSSC-NS-NW, DSSC-HS-NW, and DSSC-VS-NW. Another key parameter is the effect of slit orientation, comparing horizontal slits in DSSC-HS-NW and vertical slits in DSSC-VS-NW to evaluate their impact on stress concentration and load redistribution. Additionally, deformation

mechanisms are studied, with inward and outward buckling prominently observed in DSSC-HS-NW and DSSC-VS-NW, which indicates the slit orientation influences the overall failure mechanism.

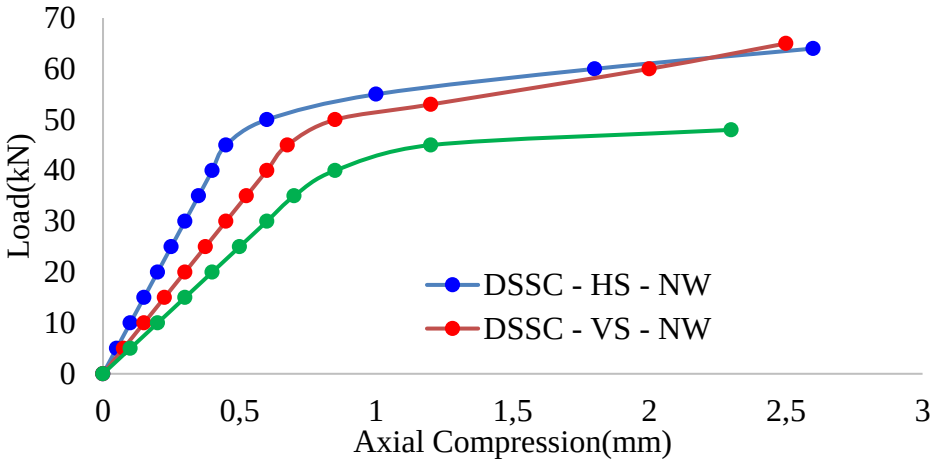

Fig. 9 Load – axial compression behavior of Group C specimens

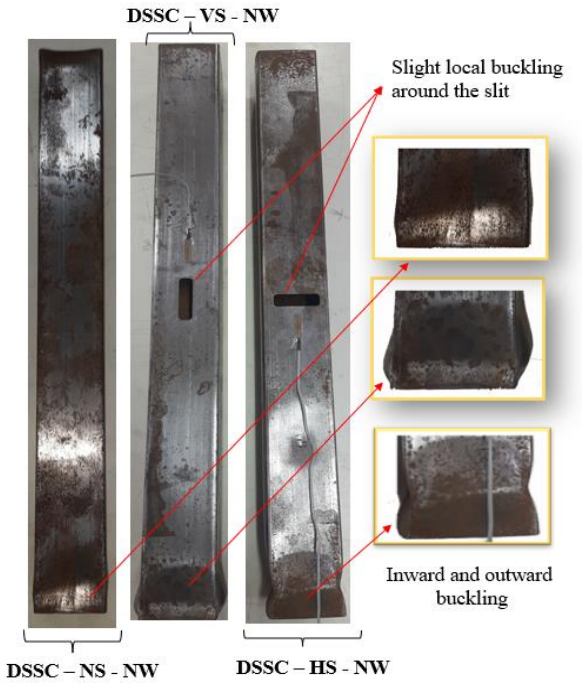

Fig. 10. Buckling pattern of the square column deficient column

3.4 Load – Axial Compression Behavior of Group D Specimens

The square hollow columns wrapped with GFRP in this study exhibited distinct behavior compared to their unwrapped counterparts. All the square columns, including DSCC-NS-GFRP, DSCC-HS-GFRP, DSCC-VS-GFRP, DSSC-NS-GFRP, DSSC-HS-GFRP, and DSSC-VS-GFRP, were strengthened by wrapping three plies of GFRP sheets using epoxy resin. Figure 11 illustrates the load-axial compression behavior of GFRP-wrapped square hollow columns with and without deficiencies. The load-carrying capacity increased significantly, with wrapped specimens showing an improvement of approximately 50%, regardless of the presence of vertical or horizontal slits. The GFRP wrapping enhanced stiffness and effectively mitigated local buckling. Notably, the confinement provided by GFRP around horizontal slits, as observed in DSCC-HS-GFRP and DSSC-HS-GFRP, was more effective than that around vertical slits, such as in DSCC-VS-GFRP and DSSC-VS-GFRP, attributed to the fiber orientation aligning favorably with the stress distribution. During axial loading, tearing of

the GFRP sheets was observed in regions of local buckling and near the slit areas, indicating critical stress concentrations and localized failure and it is shown in Fig. 12.

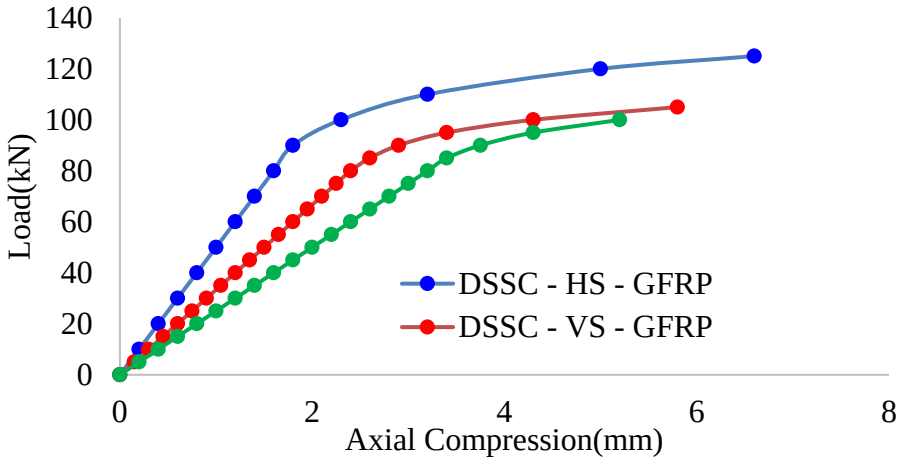

Fig. 11. Load – axial compression behavior of square Group D specimens

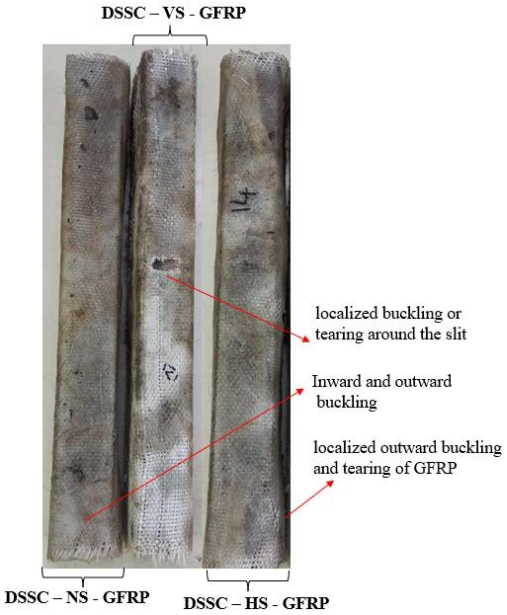

Fig. 12. Failure mode of the square hollow deficient column with GFRP wrapping

3.5 Effect of GFRP wrapping

Bar chart comparison between the unwrapped and 3 plies of GFRP-wrapped deficient column with no slit, horizontal slit and vertical slit for the circular and square section was shown in Fig. 13. From the chat it was noted that a percentage increase in the load carrying capacity of GFRP wrapped specimen is approximately twice than that of unwrapped specimen. Thus, the confinement using GFRP is found to be an effective repair technique for deficient hollow pipes/tubes. It is also observed that the circular section was found to be more effective for wrapping than the square due to the presence of the edges. GFRP wrapping on the square column will be effective with the provision of a small corner radius.

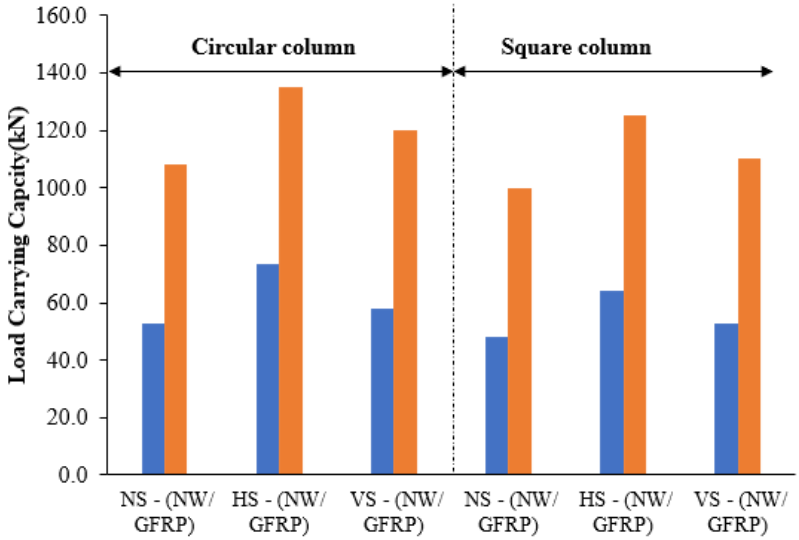

Fig. 13. Loading carrying capacity of wrapped and unwrapped deficient column

3.6 Compression Between the Experimental and FEA Model

The FEA models developed in this study can predict the failure as similar to that of experimental failure. The circular hollow column specimen and square hollow column without wrapping fail mainly by local buckling, yielding and inward and outward bucking respectively [14]. The comparison between the failure of the experimental and FEA model is illustrated in Fig. 14 & Fig.15. The colored regions in the FEA analysis (Fig.14) reveal stress patterns and failure mechanisms in circular hollow columns. For unwrapped specimens (DSCC-NS-NW, DSCC-VS-NW, and DSCC-HS-NW), red zones indicate stress concentrations and local buckling, with horizontal slits (DSCC-HS-NW) showing the most severe stress disruption. Wrapped specimens (DSCC-NS-GFRP, DSCC-VS-GFRP, and DSCC-HS-GFRP) exhibit more uniform stress distribution, delayed buckling, and reduced stress intensities near slits. GFRP wrapping is particularly effective in confining stress around horizontal slits due to fiber alignment, enhancing load capacity and mitigating failure. Similarly, FEA model for deficient hollow steel square columns was compared with or without GFRP wrapping (Fig.15).

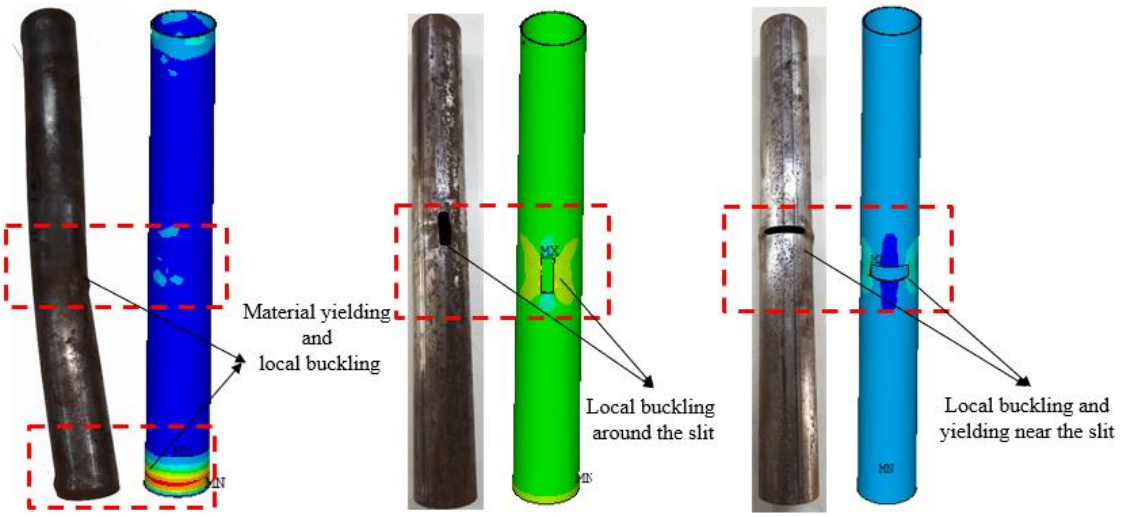

(a)DSCC-NS-NW (b) DSCC-VS-NW (c) DSCC-HS-NW

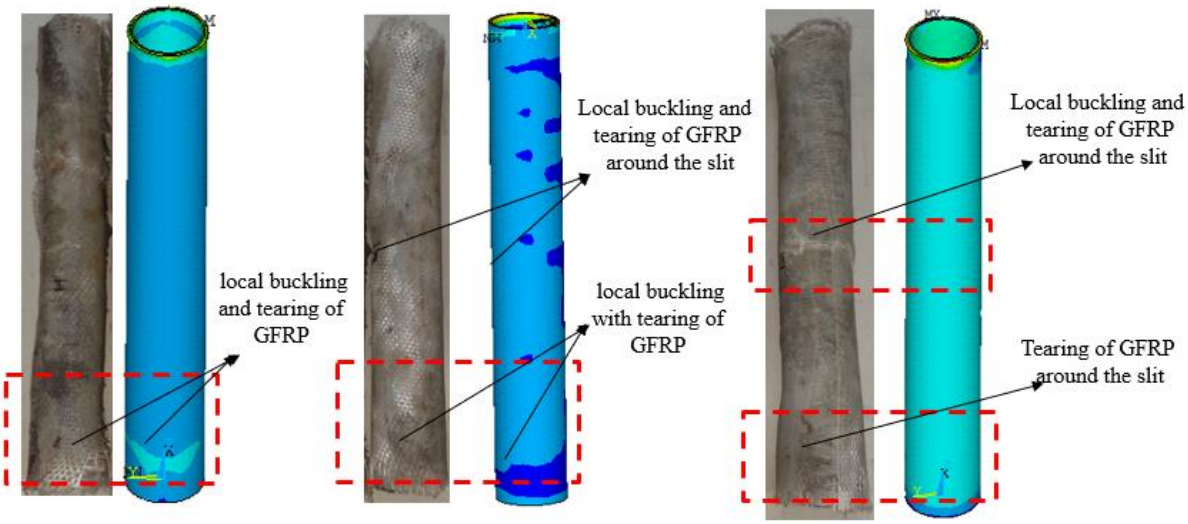

(d) DSCC-NS-GFRP (e) DSCC-VS-GFRP (f) DSCC-HS-GFRP

Fig. 14. Comparison between the failure mode of Experimental and FEA model of circular hollow column

In DSSC-NS-NW, the red zones at the middle and bottom of the column correspond to material yielding and localized inward and outward buckling. In DSSC-HS-NW (horizontal slit), the stress is concentrated around the slit, with local inward and outward buckling forming due to stress redistribution. The DSSC-VS-NW (vertical slit) specimen shows stress concentration along the slit edges, leading to local buckling near the slit. Whereas in DSSC-NS-GFRP, the stress distribution is more uniform, and localized buckling is delayed due to the confinement provided by the GFRP. The DSSC-VS-GFRP specimen shows improved stress redistribution around the vertical slit, with reduced buckling intensity compared to the unwrapped columns. From Fig.14 & Fig.15, it was observed that a good correlation between the experimental and numerical models was achieved.

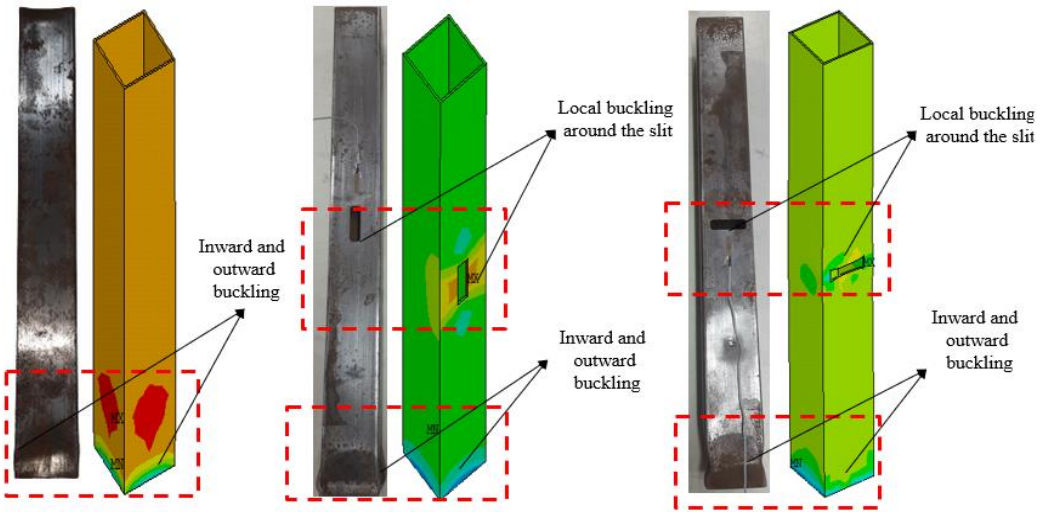

(a) DSSC-NS-NW (b) DSSC-VS-NW (c) DSSC-HS-NW

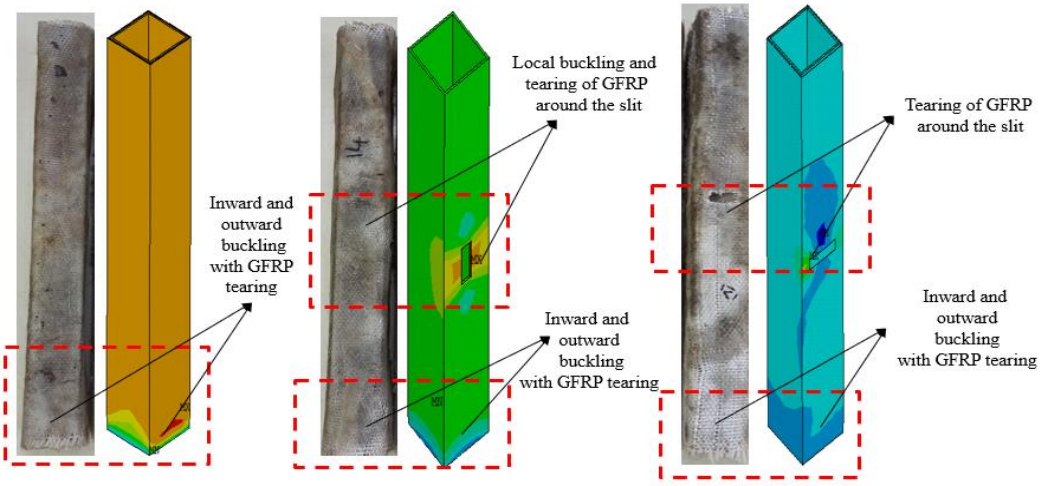

(d) DSSC-NS-GFRP (e) DSSC-VS-GFRP (f) DSSC-HS-GFRP

Fig. 15. Comparison between the failure mode of Experimental and FEA model square hollow column

3.7 Strength of Hollow Deficient Column with or Without GFRP Wrapping As Per AISI Code

The design strength of steel columns without GFRP wrapping is calculated using the provisions of AISI-S100[15], which provides a well-established framework for evaluating the axial load-carrying capacity of cold-formed steel members. The equations in AISI-S100 consider nominal material properties, such as the yield strength (F_y), and geometric characteristics, including effective cross-sectional area (A_e) and slenderness effects. For columns, the design strength (N_{AISI}) is determined based on whether the column slenderness (λc) falls within the inelastic or elastic buckling range, as defined by the critical slenderness parameter. These calculations provide a baseline strength for steel columns without external reinforcement. When GFRP wraps are introduced, the confinement effect and additional strength provided by the composite material lead to a significant enhancement in the column's load-carrying capacity. The contribution of GFRP wrapping is quantified by comparing the experimentally or numerically determined ultimate strength of the wrapped column to the unwrapped column's baseline strength calculated using AISI-S100. This approach highlights the strengthening effect of GFRP wraps and validates their efficiency in improving the performance of steel columns under axial loads. The design strengths are calculated using AISI - S100 [15] for steel hollow columns were calculated using Eq. [1-4]. The strength obtained from the experimental, FEA model and AISI design equation are summarized in Table 3.

$$N_{AISI} = A_e P_n \tag{1}$$

$$P_n = \left(0.658^{\lambda_c{}^2}\right) F_y \; for \; \lambda_c \leq 1.5 \tag{2}$$

$$P_n = \left(\frac{0.877}{\lambda_c{}^2}\right) F_y \; for \; \lambda_c > 1.5 \tag{3}$$

$$\lambda_c = \sqrt{\frac{F_y}{F_e}} \tag{4}$$

The strength of the column obtained from the FEA model overestimates by 3.5% as compared to experimental values. The FEA model tends to overestimate strength due to idealized material properties, assumptions of perfect bonding, and the omission of real-world imperfections such as geometric flaws and progressive damage. The mean and coefficient of variance between the N_{EXP} and N_{FEA} are 0.97 and 0.014 respectively. From Table 2, it was also found that the strength calculated using AISI for the hollow deficient column was 12.7**%** lower than experimental results due to its conservative approach and simplified assumptions made as ideal material properties.

The design strength was also calculated without considering the confinement effect of GFRP wrapping on the hollow column with or without vertical and horizontal slits. The mean and coefficient of variance between the N_{EXP} and N_{AISI} are 1.15 and 0.045 respectively.

Table 3. Comparison between hollow column strength of Experimental, FEA and AISI

Specimen	Ultimate Load			$\frac{N_{EXP}}{N_{FEA}}$	$\frac{N_{EXP}}{N_{AISI}}$
	N_{EXP} (kN)	N_{FEA} (kN)	N_{AISI} (kN)		
DSCC-NS-NW	53.2	55.3	46.4	0.96	1.14
DSCC-HS-NW	73.6	75.3	58.9	0.98	1.25
DSCC-VS-NW	58.1	59.5	52.3	0.98	1.11
DSCC-NS-GFRP	108.2	112.2	94.0	0.96	1.15
DSCC-HS-GFRP	135.3	139.5	120.2	0.97	1.12
DSCC-VS-GFRP	120.2	125.4	105.0	0.96	1.14
DSSC-NS-NW	48.7	51.3	41.3	0.94	1.16
DSSC-HS-NW	64.5	67.2	57.6	0.96	1.11
DSSC-VS-NW	53.2	54.2	47.7	0.98	1.11
DSSC-NS- GFRP	100.2	102.3	91.0	0.98	1.10
DSSC-HS- GFRP	125.9	127.2	112.5	0.98	1.11
DSSC-VS- GFRP	110.3	112.1	88.0	0.98	1.25
Mean				0.97	1.15
COV				0.014	0.045

4. Conclusions

Based on the experimental and FEA investigations, the following specific conclusions are drawn:

- The presence of vertical and horizontal slits in circular hollow steel columns (DSCC specimens) and square hollow steel columns (DSSC specimens) results in a redistribution of stress, altering the load path and influencing the local buckling around the slit edges. The axial load-carrying capacity of unwrapped DSCC-NS-NW and DSSC-NS-NW specimens was 53.0 kN and 48.0 kN, respectively. The reduction in capacity was attributed to localized stress concentrations around the slit edges.
- Columns with vertical slits (e.g., DSCC-VS-NW and DSSC-VS-NW) showed greater reductions in axial load capacity (by 9.2% and 10.4%, respectively, compared to their horizontal slit counterparts) due to the stress redistribution along the column height, which intensifies buckling behavior.
- GFRP wrapping significantly improved axial strength and stiffness in deficient columns. For example, the DSCC-NS-GFRP column exhibited a 103.8% increase in axial load capacity compared to its unwrapped counterpart, reaching 108.0 kN. Similarly, DSSC-NS-GFRP showed an increase of 108.3%, reaching 100.0 kN. The three-ply GFRP wrapping redistributed stresses effectively, delayed local buckling, and enhanced ductility by preventing sudden failure
- Failure mechanisms of unwrapped columns differ by geometry: unwrapped circular columns failed by localized material yielding and buckling near the slit, while square columns exhibited inward and outward buckling at the slit. In GFRP-wrapped columns, failure modes transitioned to delamination, tearing of the GFRP sheets, and combined global and local buckling, as observed in DSCC-HS-GFRP and DSSC-HS-GFRP specimens.
- The FEA model predicted the load-carrying capacities of hollow deficient columns with high accuracy, showing a minimal error of 3.5% when compared to experimental results. For instance, the predicted capacities for DSCC-NS-NW and DSSC-NS-NW were 51.3 kN and 46.3 kN, closely matching experimental results of 53.0 kN and 48.0 kN, respectively.
- The AISI estimates for load-carrying capacities were conservative, with predictions 12.7% lower than experimental results. For example, the estimated capacity for DSSC-NS-GFRP was 87.3 kN, compared to the experimental value of 100.0 kN. This conservatism highlights the

need for further refinement of AISI guidelines when considering hollow deficient columns with or without GFRP wrapping.

These findings underline the significant role of slit orientation, geometry, and GFRP confinement in governing the axial load capacity and failure modes of hollow steel columns, providing a reliable experimental and numerical foundation for future design improvements.

List of Notations

HSC	Hollow steel column
DSCC	Deficient Steel circular column
DSSC	Deficient steel square column
NS	No slit
VS	Vertical slit
HS	Horizontal slit
NW	No wrap
GFRP	Glass fiber-reinforced polymer
CFRP	Carbon fiber reinforced polymer
UTM	Universal testing machine
FEA	Finite element analysis
N_{AISI}	Design strength in kN
N_{Exp}	Experimental strength in kN
N_{FEA}	Numerical strength in kN

Appendix

1. Determine the critical slenderness ratio (λ_c):

$$\lambda_c = \sqrt{\frac{F_y}{F_e}}$$

Where; F_y: Yield strength of steel (assumed 257 MPa or N/mm^2), F_e: Elastic buckling stress derived using Euler's formula.

The elastic buckling stress Fe is given as:

$$F_e = \frac{\pi^2 E}{\left(\frac{KL}{r}\right)^2}$$

For simplicity in the AISI equation, λ_c is already pre-calculated as an input parameter, based on geometry and material properties.

2. Use appropriate P_n equations

From the AISI-S100 design standards:

For $\lambda_c \leq 1.5$*:*

$$P_n = (0.658^{(\lambda c)^2}) F_y$$

For $\lambda_c \geq 1.5$*:*

$$P_n = \left(\frac{0.877}{\lambda c^2}\right) F_y$$

3. Calculated the net area (A_c)

D= 76.5mm (Outer diameter)

t_s = 1.8mm (thickness)

$$A_c = \frac{\pi(76.5-2(1.8))^2}{4} = \frac{\pi(72.9)^2}{4} = 4177.25\ mm^2$$

4. Calculate nominal axial strength (P_n)

Given F_y = 257 N/mm² and assuming $\lambda_c \leq 1.5$ for this specimen:

$$P_n = (0.658^{(\lambda c)^2}) F_y$$

Use, $(\lambda c)^2 = 1.2$ (example for DSCC-VS-GFRP)

$$P_n = (0.658)^{1.2} \times 257 = 0.490 \times 257 = 125.93 \text{ N/mm}^2$$

5. Calculate the ultimate strength from AISI formula:

Using $N_{AISI} = A_c . P_n$:

$N_{AISI} = 4177.25 \times 125.93 = 105.0$ KN

6. Compare experimental strength from AISI formula:

Specimen	N_{EXP} (KN)	N_{FEA}(KN)	N_{AISI}(KN)	N_{EXP}/N_{FEA}	N_{EXP}/N_{AISI}
DSCC-VS-GFRP	120.2	125.4	105.0	0.96	1.14

Acknowledgement

The authors would like to thank the management of Sri Siva Subramaniya Nadar College of Engineering for giving the needed facilities to complete this research work.

References

[1] Ghaemdoust MR, Narmashiri K, Yousefi O. Structural behaviours of deficient steel SHS short columns strengthened using CFRP. Constr Build Mater. 2016;126:1002-1011. https://doi.org/10.1016/j.conbuildmat.2016.09.099

[2] Rao S, Kumar P, Singh R. Strengthening of hollow steel columns using glass fiber reinforced polymer. J Struct Eng. 2017;143(3):04016206.

[3] Shahraki M, Sohrabi MR, Azizyan GR, Narmashiri K. Strengthening of deficient steel SHS columns under axial compressive loads using CFRP. Steel Compos Struct. 2019;30(1):69-79.

[4] Ghaemdoust MR, Narmashiri K, Yousefi O. Structural behaviors of deficient steel SHS short columns strengthened using CFRP. Constr Build Mater. 2016;126:1002-1011. https://doi.org/10.1016/j.conbuildmat.2016.09.099

[5] Shahraki M, Sohrabi MR, Azizyan GR, Narmashiri K. Experimental and numerical investigation of strengthened deficient steel SHS columns under axial compressive loads. Struct Eng Mech. 2018;67(2):207-217.

[6] Lin J, Wang C, Xu J. Comparative study on the strengthening of hollow steel columns using steel plates and GFRP. Thin-Walled Struct. 2019;144:106286.

[7] Sangeetha P, Sumathi R. Behaviour of glass fibre wrapped concrete columns under uniaxial compression. Int J Adv Eng Technol. 2010;1(1):74-83.

[8] Palanivelu S, Moorthy D, Subramani G, Dhayanithi JR. Strength enhancement of cold-formed steel tubular column using GFRP strip subjected to axial compression. Građev Mater Konstrukcije. 2021;64(4):251-260. https://doi.org/10.5937/GRMK2104251P

[9] Shahraki M, Darmiyan HM. Structural behaviours of strengthened deficient steel square hollow section columns under axial compressive loads. Innov Infrastruct Solut. 2023;8:1-13. https://doi.org/10.1007/s41062-022-00955-0

[10] Tang H, Liu R, Zhao X. Axial compression behaviour of CFRP-confined rectangular concrete-filled stainless steel tube stub column. Front Struct Civ Eng. 2021;15:144-1159. https://doi.org/10.1007/s11709-021-0762-4

[11] Keykha AH. Carbon-fibre strengthening of deficient hollow steel sections under combined loading. Proc Inst Civ Eng Struct Build. 2019;172(8):609-620. https://doi.org/10.1680/jstbu.17.00150

[12] Sharma A, Singh P. Finite element analysis of GFRP-strengthened hollow steel columns with slits. J Constr Steel Res. 2020;170:106169.

[13] Latour M, Di Benedetto S, Francavilla AB, Elettore G, Rizzano G. Stiffness and strength of square hollow section tubes under localised transverse actions. Metals. 2023;13(10):1767. https://doi.org/10.3390/met13101767

[14] Sangeetha P. Analysis of FRP wrapped concrete columns under uniaxial compression. J Sci Ind Res. 2007;66(3):235-242.

[15] American Iron and Steel Institute (AISI). Specification for the design of cold-formed steel structural members. AISI S100-2007. 2007.